High-Temperature Flow Stress and Recrystallization Characteristics of Al-Bearing Microalloyed TWIP Steels

MAHESH CHANDRA SOMANI, DAVID A. PORTER, ATEF S. HAMADA, and L. PENTTI KARJALAINEN

In this study, the effects of microalloying (Nb,V) and aluminum on the constitutive flow behavior and static recrystallization (SRX) characteristics of microalloyed TWIP steels (Fe-20Mn-0.6C-Al-(Nb,V)) have been investigated under hot deformation conditions. Compression tests in a Gleeble simulator, including the double-hit technique, enabled the acquisition of flow stress and recrystallization data. These were analyzed to determine the powers of strain and strain rate as well as the activation energies of deformation and recrystallization (Q_{def} and Q_{rex}). Aluminum increased the flow stress and activation energy of deformation and delayed the onset of dynamic recrystallization of microalloyed TWIP steels. While microalloying with V up to 0.3 pct seems to have little or no effect on the SRX kinetics, microalloying with 0.026 pct Nb significantly slowed down the SRX rate, similarly as in the case of low C-Mn steels. Addition of high aluminum (4.9 pct) marginally retarded the SRX kinetics in comparison with the steels with low aluminum (1.5 pct), with or without microalloying with V.

I. INTRODUCTION

EXTENSIVE efforts have been directed in recent years to improve the fuel efficiency and crash worthiness of automobiles through the development of advanced light-weight, high-strength steel sheets with excellent ductility. Notable among the new developments are the austenitic steels with 16 to 25 pct Mn that exhibit enhanced ductility and energy absorption ability through twinning-induced plasticity (TWIP).[1–3] The yield strength of austenitic TWIP steels with 16 to 25 pct Mn is relatively low, below ≈400 MPa, and therefore new efforts are necessary to improve it. One obvious method is to refine the grain size that can result in a significant increase of yield strength or alternatively, prestraining of a sheet followed by recovery and partial recrystallization of that sheet.[3] It is also well known for decades that precipitation strengthening by microalloying can be used to increase the yield strength of ferritic steels, but it has not been utilized to the same extent in the case of TWIP steels. Only a couple of papers concern the improvement of the performance of high-Mn TWIP steels by increasing their yield strengths using microalloying.[3–5] Chateau et al.[4]

achieved an increase of 140 MPa owing to the precipitation of semicoherent VC precipitates below 30 nm in size in an Fe-22Mn-0.6C steel (hereinafter concentrations in wt pct, unless mentioned otherwise) with 0.21 at. pct V. Scott et al.[5] investigated precipitation strengthening in three cold-rolled and annealed TWIP steels and observed that V is the most efficient strengthening element and an increase of yield strength by about 200 MPa is realized by alloying with 0.35 pct V and even a yield strength of 900 MPa could be achieved by alloying with 1 pct V. The potentials of Ti and Nb alloying remained less pronounced. Precipitation strengthening by Nb and V in microalloyed TWIP steels has also been targeted in a recent project funded by the Research Fund for Coal and Steel (RFCS).[6]

While the influences of chemical composition on the microstructures and mechanical properties of TWIP steels at room temperature have been extensively investigated and published in the literature, the information on the constitutive flow and recrystallization behaviors of these steels at high temperatures is scarcer. Hamada et al.[7–9] have investigated high-temperature flow stress, dynamic recrystallization (DRX) and static recrystallization (SRX) behaviors of Fe-24Mn-0.10C and Fe-26Mn-3.4Al-0.14C TWIP steels in compression testing at temperatures between 1173 K to 1373 K (900 °C to 1100 °C) and strain rates 0.005 to 5 s^{-1}. They observed that both the high-Mn content of the steels and the Al alloying resulted in a significant increase in the hot deformation resistance compared with the low-carbon steel. The onsets of DRX as well as the kinetics of SRX were significantly retarded by Mn and Al alloying compared with in low-carbon steels. Li et al.[10] studied the hot deformation behavior of an

MAHESH CHANDRA SOMANI, Senior Specialist Researcher, DAVID A. PORTER, Professor and Head, and L. PENTTI KARJALAINEN, Emeritus Professor, are with the Faculty of Technology, Materials Engineering, Centre for Advanced Steels Research, University of Oulu, PO Box 4200, 90014 Oulu, Finland. Contact e-mail: mahesh.somani@oulu.fi ATEF S. HAMADA, Associate Professor, is with the Department of Metallurgical and Materials Engineering, Faculty of Petroleum and Mining Engineering, Suez University, Box 43721, Suez, Egypt.
Manuscript submitted February 16, 2015.
Article published online September 3, 2015.

Fe-0.02C-25Mn-3Si-3Al-0.02C TWIP steel in the temperature range from 1073 K to 1373 K (800 °C to 1100 °C) and strain rate range from 0.01 to 5 s^{-1} and found that DRX is the most important softening mechanism and strongly affected by temperature and strain rate. The peak stress level decreased with the increasing deformation temperature and the decreasing strain rate, which could be predicted by the Zener–Hollomon (Z) parameter in the hyperbolic sine equation. Marandi et al.[11] developed appropriate constitutive equations based on the hyperbolic sine equation by considering the related material constants as functions of strain for a TRIP/TWIP steel (Fe-21Mn-2.7 Si-1.6Al-0.11C).Similarly, Zhang et al.[12] carried out constitutive analysis of the hot deformation behavior of an Fe-23Mn-2Al-0.2C TWIP steel in the temperatures ranging from 1173 K to 1423 K (900 °C to 1150 °C) and the strain rate range of 0.001 to 20 s^{-1}. They also derived the strain-dependent constitutive equations on the basis of the hyperbolic sine relationship.

However, the effect of microalloying on hot-rolled TWIP steels has been investigated even more scarcely. Reyes et al.[13] found that microalloyed TWIP steels (Fe-22Mn-1.6Al-1.4Si-0.4C; 0.06Nb, 0.18Ti, 0.12V) tested at 1373 K (1100 °C) and low strain rate (10^{-4} s^{-1}) had higher peak stress values than the non-microalloyed TWIP steel, but they experienced a reduction of the peak strain values. Microalloying elements Nb, V, and Ti had a significant influence on the activation energy of deformation (Q_{def}) thus resulting in an increase by 19, 22, and 16 pct, respectively, in comparison with the non-microalloyed steel. Dobrzański and Borek[14,15] investigated the hot deformation behaviors of two TWIP steels, Fe-26Mn-3Si-3Al-0.033Nb-0.009Ti and Fe-27Mn-4Si-2Al-0.033Nb-0.009Ti. Both steels had similar behavior, the values of flow stress varied from 250 to 450 MPa at temperatures ranging from 1323 K to 1123 K(1050 °C to 850 °C) (strain rate 10 s^{-1}), increasing with the decreasing deformation temperature. These values are essentially higher compared with conventional C-Mn and microalloyed steels. Schinhammer et al.[16] studied the interplay between recrystallization and precipitation during annealing of a cold-rolled biodegradable TWIP Fe-21Mn-0.7C-1Pd steel. The very fine Pd-rich precipitates that formed in the deformed matrix were found to suppress the onset of recrystallization.

Due to strengthening advantages of microalloying of TWIP steels, there is a need for further studies on its influence on high-temperature behavior of TWIP steels, and hence this paper presents a summary of the constitutive flow behavior with determination of Q_{def} and analysis of SRX kinetics of select Al-bearing Nb or V-microalloyed TWIP steels under hot deformation conditions. The constitutive flow is based on the exponent-type equation proposed by Sellars and Tegart.[17] SRX characteristics were evaluated and kinetics modeled using a fractional softening approach together with metallography to determine the time for 50 pct recrystallization as a function of strain, strain rate, grain-size, and temperature by applying double-hit compression tests using a Gleeble 1500 thermomechanical simulator.

The SRX fractional softening equations were developed including measurements of powers of strain and strain rate exponents and activation energy of recrystallization (Q_{rex}), in accordance with the regression modeling performed previously by Somani et al.[18,19] for various steels. Some examples of verification of the regression equation and further comparison of the kinetics with those of other steels including C-Mn, Nb-microalloyed, austenitic stainless and ordinary TWIP steels are also presented in this paper.

II. EXPERIMENTAL

A. Approach and Materials

The experimental TWIP steels with controlled additions of C, Mn, Al with or without microalloying elements Nb or V were supplied by ThyssenKrupp Steel Europe AG (TKSE), Germany. The experimental steels were cast and homogenized prior to rolling at a pilot plant of TKSE. Suitable defect-free samples of about 12-mm thickness were extracted between the surface and the center of the rolled plates for further studies at the University of Oulu. Of the various experimental steels received in the hot-rolled condition, four 0.6C-20Mn-Al-(Nb/V) steels, viz., TKSE 4, TKSE 12, TKSE 16, and TKSE 18 were selected for investigation in this work and their compositions are presented in Table I. Steel TKSE 4 bearing low Al (1.5 pct) is free from any microalloying element and is used in this study as the reference steel for comparison. All other steels are microalloyed with either 0.026 pct Nb (TKSE 12) or 0.3 pct V(TKSE 16 and 18). To understand the effect of Al on SRX rate, both low (1.5 pct) and high (~5 pct) levels of Al were tried in V-microalloyed steels (TKSE 16 and 18, respectively, Table I).

B. Hot Compression Tests

Bars of 12 × 12-mm cross section cut from the rolled plates were solution treated at 1493 K (1220 °C) for 10 minutes under argon atmosphere in order to dissolve the microalloying elements followed by quenching in water. Cylindrical specimens of ∅8 × 10 mm were machined for compression testing with their axes parallel to the rolling direction and plane. Axisymmetric hot compression tests were carried out on a Gleeble 1500 thermomechanical simulator. A graphite foil was inserted between the cylindrical specimen and the tungsten carbide compression anvils to reduce the friction and a tantalum foil to prevent sticking with the anvils. These foils, owing to their low electrical conductivity compared with steel, also keep the longitudinal temperature gradient present in the specimen to a minimum. Low friction is also randomly checked and controlled by measuring the barreling of the specimens after compression, as specified in the recommended procedure.[20] This showed that no correction for friction is required for strains up to approximately 0.8. Adiabatic heating as a consequence of hot deformation can influence the flow behavior, noticeably at low

Table I. Compositions of the High-Mn Steels Along with Their Precipitate Dissolution Temperatures[6]

Steel Code	C	Mn	Al	V	Nb	Fe	VC/NbC Dissolution Temp. [K (°C)]
TKSE 4	0.61	20.6	1.5	0.00	0.00	bal.	—
TKSE 12	0.61	20.1	1.6	0.00	0.026	bal.	≈1453 (1180)
TKSE 16	0.60	20.0	1.5	0.30	0.00	bal.	≈1238 (965)
TKSE 18	0.62	20.4	4.9	0.31	0.00	bal.	≈1243 (970)

temperatures and high strain rates. In Gleeble simulator, the temperature of the specimen is measured and controlled by a thermocouple, welded on the surface, so that the specimen temperature is ultimately controlled by a high-speed computerized system tending to prevent any adiabatic temperature rise by suitably varying the instantaneous power input to the system. However, at the highest strain rate used (5 s^{-1}), the control rate is not good enough, and some rise in temperature is unavoidable.

In order to understand the constitutive flow stress behavior, the specimens were reheated in vacuum at 10 K/s (10 °C/s) to 1473 K (1200 °C), held for 1 minute, followed by cooling at 5 K/s (5 °C/s) to the test temperatures ranging from 1223 K to 1373 K (950 °C to 1100 °C). After soaking the specimens for 10 seconds at the test temperature, the specimens were compressed to a true strain of 0.8 at constant true strain rates ranging from 0.01 to 5 s^{-1}.

C. Double-Hit Compression Tests

As with other highly alloyed TWIP and stainless steels,[9,21,22] the stress relaxation technique was found to be unsuitable for the steels in the current study to determine SRX kinetics. Therefore, the SRX kinetics of the four steels, as given in Table I, were studied by employing the double-hit compression technique at temperatures ranging from 1223 K to 1373 K (950 °C to 1100 °C) and at different strains (0.125 to 0.3) and strain rates (0.01 to 5 s^{-1}). The applied strain during second hit was 0.2, and the holding times between the two compression hits were ranging from 1 to 1000 seconds. The typical test schedule is shown in Figure 1. In order to exclude the effect of recovery from the softening data the flow stress at 5 pct total reloading strain was adopted in computing the recrystallized fraction, as described elsewhere.[21,22]

The corresponding grain sizes estimated by linear intercept method for the four TKSE steels following reheating at 1423 K (1150 °C) for 2 minutes are given in Table II [hence, this is the grain size inherited from initial solution treatment at 1493 K (1220 °C) for 10 minutes]. As per the test plan, some specimens from each steel were reheated at 1523 K (1250 °C) for 5 minutes prior to double-hit compression testing in order to produce relatively coarse grain structure for favor of understanding the influence of grain size on SRX kinetics. The corresponding grain sizes are also included in Table II. Even though the grain sizes at lower reheating temperature of 1423 K (1150 °C) are not really fine, typically ranging from 90 to 160 μm (Table II), these are so termed here solely for the purpose of comparison. As expected,
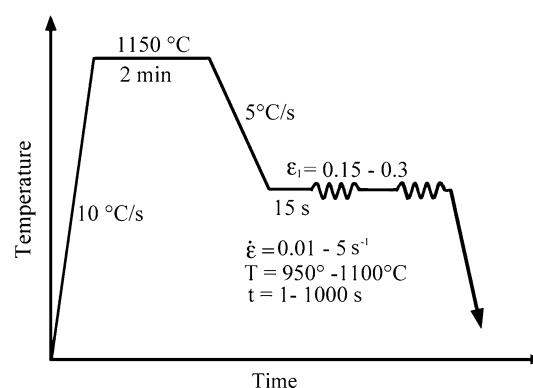

Fig. 1—Test schedule used in double-hit compression tests.

Table II. Average Grain Size of the Investigated Steels After Reheating at Different Temperatures Prior to Double-Hit Compression Testing

Steel	Reheating Conditions*		GS (μm)
	Temperature [K (°C)]	Time (min)	
TKSE 4	1423 (1150)	2	160
	1523 (1250)	5	430
TKSE 12	1423 (1150)	2	90
	1523 (1250)	5	240
TKSE 16	1423 (1150)	2	110
	1523 (1250)	5	260
TKSE 18	1423 (1150)	2	120
	1523 (1250)	5	300

*Samples subjected to homogenization treatment at 1493 K (1220 °C)/10 min prior to reheating in Gleeble simulator.

microalloyed steels TKSE 12, 16, and 18 show relatively finer grain structure in comparison with the non-microalloyed reference steel TKSE 4. The difference in grain sizes between the coarse and fine grains ranges from 2.4 to 2.7 times.

Using light optical microscopy, it was difficult to definitively distinguish deformed (slightly pancaked) grains from partially recrystallized grains after the first hit. Therefore, recrystallized fractions in TKSE 12 were determined from the EBSD orientation maps recorded using a Zeiss ULTRA *plus* field emission scanning electron microscope. The TKSE 12 specimens were deformed at 1373 K (1100 °C) to a strain of 0.2 at 0.1 s^{-1} and held for 2 and 30 seconds before water quenching to room temperature and sectioning parallel to the compression axis. An operating voltage of 15 kV, probe current of ~10 nA, and a step size of 0.1 μm were employed. The working distance was maintained at

~15 mm with a specimen tilt angle of 70 deg. The indexed pixels were ranging from 90 to 96 pct. Following the acquisition, the majority of non-indexed pixels was cleaned by enhancing the image, *i.e.*, filling them up with the surrounding orientations. Recrystallized fractions were determined using the Tango®* software of Oxford instruments plc.

---

*Tango® is a registered trademark of Oxford Instruments plc, Abingdon, Oxfordshire, UK.

III. RESULTS AND DISCUSSION

A. Carbide Dissolution Temperature

All the experimental steels in this study are relatively C-rich (0.6 pctC) and the VC/NbC dissolution temperatures of the microalloyed steels, *viz*. TKSE 12, 16, and 18, were calculated based on the solubility products given by the following equations, suggested in PreCHiMn version 3 (PHMN3) database[6] for the microalloyed TWIP steels by RWTH, Aachen, Germany:

$$\text{Log}[Nb][C] = 4.196 - 8703/T, \qquad [1]$$

$$\text{Log}[V][C] = 4.237 - 6157/T, \qquad [2]$$

where [Nb], [V], *etc.* are the concentrations of respective elements in weight percent, and T is the absolute temperature (in K). The calculated dissolution temperatures for different microalloyed steels are also included in Table I. The solubility product for VC given by Eq. [2] is somewhat lower than the solubility product predictions [≈1273 K (≈1000 °C)] of Multipreci model developed by ArcelorMittal[23] and ThermoCalc calculations.[24] Anyhow, from the dissolution temperatures, we can conclude that NbC tends to precipitate at all deformation temperatures applied here and VC at temperatures of ≈1243 K (≈970 °C) and below.

B. Flow Stress Behavior

Examples of typical true stress–true strain curves obtained under various hot deformation conditions are presented in Figure 2. TKSE 18 with a high Al content (4.9 wt pct) showed a slightly higher flow resistance than both steels TKSE 16 and TKSE 12 bearing relatively low Al content (1.5 wt pct). With the increasing strain rate and the decreasing temperature, the strengthening effect of Al becomes more significant. In agreement, Hamada *et al.*[7–9] reported that the addition of Al (up to 3 wt pct) increased the flow stress of high-Mn TWIP steels, by the strengthening coefficient of 14 MPa/wt pct Al. However, with higher Al content (>3 to 6 pct), the strengthening effect of Al was found to be weak.[8,9] Park *et al.*[25] observed that the addition of 6 pctAl into the fully austenitic Fe-22Mn-0.6C steel increased the flow stress at low strains but decreased strain hardenability under both quasistatic and dynamic high strain rate loading.[8,9] McQueen *et al.*[26] reported that Al has a high solid solution-strengthening effect in austenite (12 pct per 0.1 at. pct) in comparison with a relatively
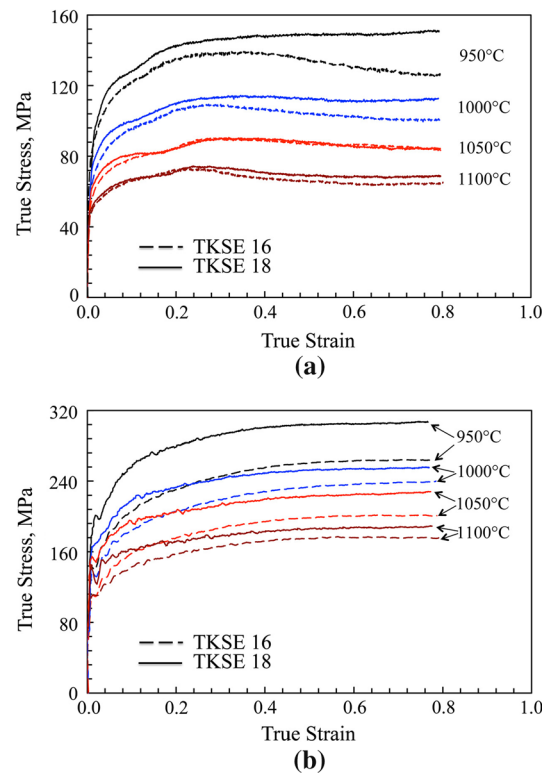

Fig. 2—Flow stress curves of TKSE 16 and TKSE 18 steels obtained at various temperatures ranging from 1223 K to 1373 K (950 °C to 1100 °C) and strain rates (*a*) 0.01 s^{-1} and (*b*) 5 s^{-1}.

weak strengthening effect of Mn (2.1 pct per 0.1 at. pct). Park *et al.*[25] suggested the increase of flow stress is due to the suppression of mechanical twinning by Al addition that increases the stacking fault energy of high-Mn austenite.

Microalloying with Nb or V did not show any discernible effect on flow stress level in these highly alloyed steels, in accordance with that observed in the case of carbon steels, too.[22] Reyes-Calderón *et al.*[13,27] studied the effect of microalloying elements such as 0.06Nb, 0.12V, and 0.18Ti on the hot flow behavior of high-Mn TWIP steels. They reported that these contents of microalloying elements have only an insignificant influence on the flow stress at high temperatures. Earlier, it has been shown that the flow stress of both Nb-microalloyed carbon steel as well as Type 304 steel remained lower than that of the microalloyed TWIP steel.[28]

At the strain rate of 0.01 s^{-1} (Figure 2(a)), a small peak can be detected in the flow stress curves of TKSE 16 at all test temperatures indicating the occurrence of DRX. However, a broad peak stress behavior was generally noticed in the flow stress curves of TKSE 18. It is seen that Al alloying delays the onset of DRX, in concurrence with the results reported earlier.[8] With the increasing strain rate and the decreasing temperature, the strengthening effect of aluminum becomes more obvious, Figure 2(b). Hamada *et al.*[7,8] found that both high-Mn and Al contents in TWIP steels retard the onset of DRX considerably compared with low-carbon

steels. However, in the current study, it is difficult to exclude the influence of microalloying elements V or Nb on the peak stress behavior, whereas the variation in grain-size, and/or Al content may also have influences on the result. However, Reyes et al.[13] reported that DRX fraction and recrystallized grain size decrease due to V microalloying.

C. Activation Energy of Deformation (Q_{def})

The hyperbolic sine law is a universal equation suitable for a wide stress range and therefore extensively used to describe the hot deformation behavior of metals including TWIP steels.[10–12,27] However, the exponent-type equation proposed by Sellars and Tegart[17] is also used to represent the correlation between the peak flow stress (σ_p), especially for relatively low stresses, and the strain rate (ε') and temperature (T, in K), as given by Eq. [3]:

$$\sigma_p = A[\varepsilon' \exp(Q_{def}/RT)]^m, \qquad [3]$$

where m is the strain rate sensitivity of flow stress, R is the gas constant, and A is a material-dependent constant. Flow stress data obtained at different temperatures and strain rates were used to determine Q_{def} and the strain rate sensitivity of the flow stress (m). Peak stress (σ_p) data and corresponding peak strains (ε_p) measured from the flow stress curves at different temperatures ranging from 1223 K to 1373 K (950 °C to 1100 °C) and strain rates (0.01 to 5 s^{-1}) are presented in Table III. In some cases, particularly at low temperatures 1223 K (950 °C) and high strain rates (1 to 5 s^{-1}), peak strains were not reached even at a maximum strain of ≈ 0.8 imposed on all the test specimens. However, it was expected that the peak stress values will not be very different from that recorded at the maximum strain keeping in view nearly flat nature of the curves. The

temperature and strain rate dependences of the peak stress were plotted based on Eq. [3]; examples of such plots for steels TKSE 12 and 18 are shown in Figure 3.

The calculated activation energies for the hot deformation and other parameters of the constitutive equation of all studied steels are shown in Table IV together
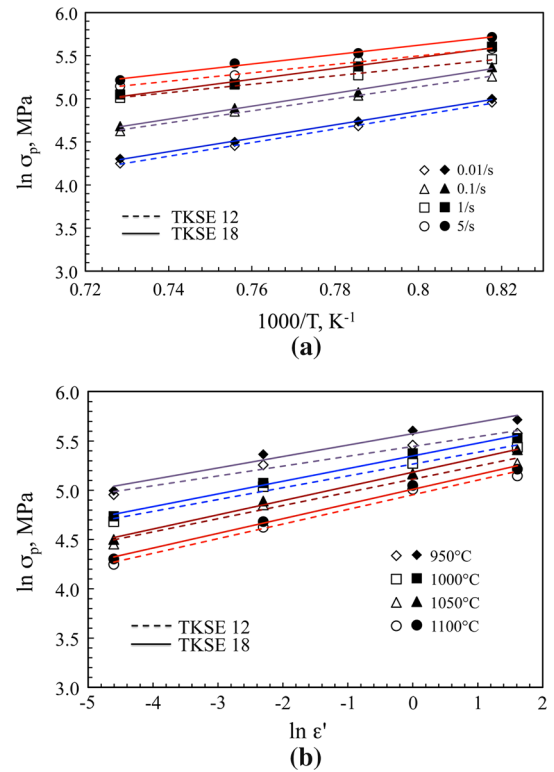
Fig. 3—Temperature (*a*) and strain rate (*b*) dependences of the peak stress used in the calculation of the activation energy of hot deformation (Q_{def}) and the strain rate sensitivity of flow stress (m), respectively.

Table III. Peak Stress (σ_p) Data and Corresponding Peak Strain (ε_p) Values Measured from the Flow Stress Curves at Different Temperatures and Strain Rates

Steel	Temp. [K (°C)] Strain Rate (s^{-1})	1223 K (950 °C) ε_p	σ_p (MPa)	1273 K (1000 °C) ε_p	σ_p (MPa)	1323 K (1050 °C) ε_p	σ_p (MPa)	1373 K (1100 °C) ε_p	σ_p (MPa)
TKSE 4	0.01	0.347	130	0.23	115	0.236	87	0.216	70
	0.1	0.5	183	0.512	155	0.44	129	0.318	103
	1	≈0.79	232	0.77	202	0.691	172	0.61	147
	5	*	260	0.796	224	0.751	196	0.72	168
TKSE 12	0.01	0.592	142	0.32	108	0.29	86	0.25	70
	0.1	0.73	192	0.557	154	0.423	128	0.333	102
	1	*	235	0.775	195	0.75	175	0.705	150
	5	*	265	0.76	230	0.768	195	0.743	172
TKSE 16	0.01	0.361	138	0.274	110	0.239	94	0.225	73
	0.1	0.59	194	0.527	164	0.39	128	0.317	105
	1	*	242	0.78	208	0.624	178	0.592	148
	5	*	264	0.79	236	0.741	200	0.655	176
TKSE 18	0.01	0.529	148	0.344	114	0.315	90	0.234	74
	0.1	≈0.798	214	0.483	160	0.518	133	0.389	108
	1	*	272	0.77	216	0.703	176	0.584	156
	5	*	304	*	252	0.756	224	0.702	185

*Peak strain not reached.

Table IV. Activation Energies of Deformation (Q_{def}) and Strain Rate Sensitivities of Flow Stress (m) for the Studied High-Mn TWIP Steels

Steel	Q_{def} (kJ mol^{-1})	m	References
TKSE 4	388	0.125	Present work
TKSE 12	402	0.125	Present work
TKSE 16	404	0.127	Present work
TKSE 18	422	0.133	Present work
Fe-22Mn-1.5Al-1.5Si-0.4C-0.06Nb	434	—	[29]
Fe-22Mn-1.5Al-1.5Si-0.4C-0.12V	446	—	[29]
Fe-25Mn-(0-6)Al	380 to 405		[8,31]
Fe-20Mn-3Si-3Al-0.04C	388		[32]
Fe-25Mn-3Si-3Al-0.02C	406		[10]
Fe-21Mn-2.7Si-1.6Al-0.11C	390 to 424		[11]
Fe-23Mn-2Al-0.2C	369 to 430		[12]
Fe-23Mn-0.6C	439		[33]

with the data for microalloyed high-Mn TWIP steels taken from reference.[29] As commonly observed, the activation energies of hot deformation of the studied steels are much greater than the activation energy for self-diffusion in γ-iron (Q = 280 kJ/mol[30]). Thus, in comparison with the activation energy of reference steel TKSE 4 (388 kJ/mol), the Q_{def} values of microalloyed steels TKSE 12 and 16 (402 and 404 kJ/mol, respectively) were slightly higher and remained practically similar, irrespective of the microalloying addition (Nb or V), Table IV. In comparison, Reyes-Calderón*et al.*[29] reported somewhat higher Q_{def} values for microalloyed Fe-22Mn-1.5Al-1.5Si-0.4C TWIP steels (434 and 446 kJ/mol for Nb and V-microalloyed steels, respectively). With further increase in Al-content from 1.5 pct (TKSE 16) to 4.9 pct (TKSE 18), the Q_{def} too increased from 404 to 422 kJ/mol, concomitant to the strengthening influence Al has on the flow stress, as discussed above.

Data for Q_{def} taken from the literature[8,10–12,29,31–33] for several non-microalloyed high-Mn steels are also included in Table IV for comparison. It can be realized that all these values fall in a relatively narrow range irrespective of the chemical composition and are comparable with the Q_{def} values estimated for the present steels. Somani *et al.*[18] have earlier used a value of 400 kJ/mol for Nb/Nb-Ti microalloyed carbon steels. In comparison, Karjalainen *et al.*[34] used a value of 390 kJ/mol for a 12Cr stainless steel and Towle and Gladman[35] obtained 410 kJ/mol for Type 304 steel. Thus, the present values seem reasonable, and these have been used to estimate the activation energies of recrystallization (Q_{rex}), as shown below.

D. Static Recrystallization (SRX) Kinetics of Microalloyed TWIP Steels

In order to be able to optimize the chemistry and processing parameters of microalloyed high-Mn TWIP steels, it is of interest to understand the way in which microalloying affects flow stress and recrystallization kinetics during hot rolling. However, so far little such information has been reported, except for the SRX characteristics of Fe-25Mn-(0-8) Al TWIP steels[9] and a modular phase-transformation kinetics model employed by Mohapatra and Sahay[36] on the experimental data in Reference 9 to describe the SRX behavior during interpass times of hot deformation. In the present instance, the grain size being generally coarse (>90 μm), the data resemble the conditions during first hot-rolling passes, even though the initial structure is wrought and not cast.

SRX kinetics have been studied using a fractional softening approach together with metallography to determine the time for 50 pct recrystallization t_{50} in accordance with the modeling performed by Somani *et al.*[18,19] using the following empirical relation[37]:

$$t_{50} = A'\varepsilon^p\varepsilon'^q d^s \exp(Q_{app}/RT), \quad [4]$$

where A' is a material constant, ε is strain, ε' is strain rate, Q_{app} is the apparent activation energy of recrystallization, d is grain size, R is the gas constant, and T is absolute temperature. The material-dependent constants p, q, and s describe the powers of the strain, strain rate, and the grain size, respectively.

As stated earlier, the SRX kinetics of the four steels, as given in Table I, were studied by employing the double-hit compression technique. Perttula and Karjalainen[21,22] found that the conventional 0.2 pct offset method in double-hit compression tests reveals about 20 pct softening due to static recovery before the start of SRX. The 5 pct total strain reloading method was suggested to be superior and was adopted in determining the recrystallized fraction in order to exclude the effect of recovery from the softening data.[21] Conventionally, the softening fraction, X, is calculated from the equation:

$$X = [(\sigma_3-\sigma_2)/(\sigma_3-\sigma_1)], \quad [5]$$

where σ_1, σ_2, and σ_3 are flow stresses for completely recrystallized, partially recrystallized, and work-hardened materials, respectively. An example of the double-hit compression technique employed on Nb-steel is shown in Figure 4, where the interrupted compression tests with various interpass times (5, 20, and 40 seconds) resulted in different recrystallized fractions ($\approx$30, 50, and 75 pct, respectively), followed by continuous compression (second hit). In the double-hit compression technique, the flow stress of recrystallized
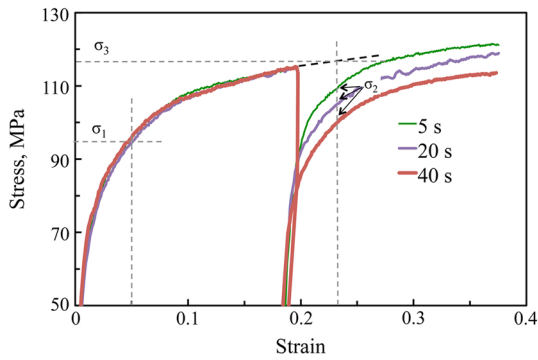
Fig. 4—An example of the double-hit compression tests conducted on a Nb-steel with different interpass times resulting in various recrystallized fractions, X.

material, σ_1 is conventionally taken from the first pass (Figure 4), although it is preferred to take it after the second pass on a completely softened material in order to avoid the possible effects of the grain size refinement on the flow stress.[21,22] The conventional method may obviously indicate somewhat lower recrystallized fractions. On the other hand, σ_3 can be obtained with reasonable accuracy by extrapolating the flow stress of the first pass. Recrystallized fractions (X) calculated at different unloading times are then fitted to the Avrami-type equations at around 50 pct recrystallization to enable an estimation of the SRX fraction as a function of holding time t:

$$X = 1 - \exp[-0.693 \times (t/t_{50})^n], \qquad [6]$$

where t_{50} is the time for 50 pct recrystallized fraction, dependent on the composition of the steel and the deformation conditions; and n is the Avrami exponent. In this way, a complete Avrami curve showing recrystallized fraction *vs* time for a given set of conditions can describe the progress of recrystallization.

1. Effects of temperature and grain size on SRX rate
Examples of SRX fractional softening data for steels TKSE 4 and TKSE 12 following deformation to 0.2 strain at 0.1 s^{-1} at four temperatures are presented in Figures 5(a) and (b). Sigmoidal Avrami-type curves can be fitted reasonably with the experimental data, although the fit is often poor for recrystallization fractions greater than those in the range from 70 to 80 pct as also noted elsewhere.[18,22] It can be seen that with the temperatures increasing from 1223 K to 1373 K (950 °C to 1100 °C), the SRX kinetics is accelerated significantly. For example, in the case of the non-microalloyed reference steel TKSE 4 (160 μm grain size), the t_{50} time shortens from 45 seconds at 1223 K (950 °C) to about 5 seconds at 1373 K (1100 °C), Figure 5(a). Data obtained on specimens reheated at 1523 K (1250 °C) for 5 minutes to produce coarser grains (430 μm) and tested at 1323 K (1050 °C) are also shown in Figure 5, which clearly reveals the retardation of recrystallization rate (t_{50} = 13 seconds) in comparison with the finer grained structure (160 μm; t_{50} = 7.5 seconds).
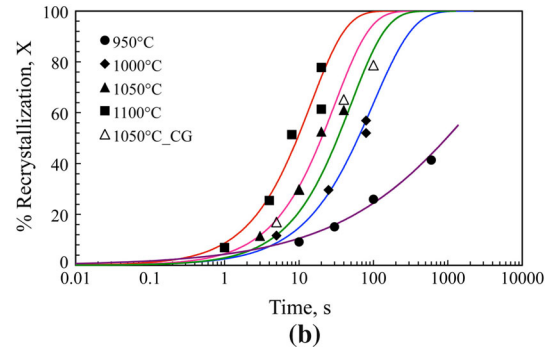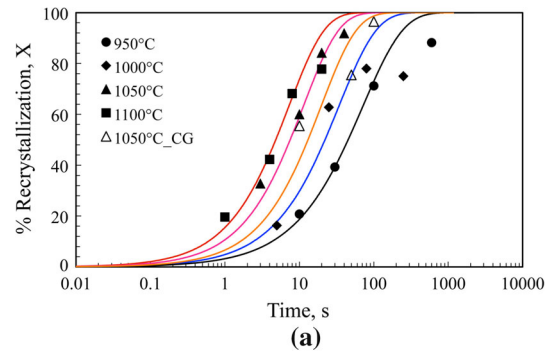

(a)

(b)

Fig. 5—Double-hit compression data fitted with Avrami-type curves showing SRX rates of steels: (*a*) TKSE 4 and (*b*) TKSE 12 at different temperatures following deformation to 0.2 strain at 0.1 s^{-1}.

Referring to Figure 5(b), it is evident that the microalloying element Nb has a significant influence on the SRX kinetics of TKSE 12. For example, at 1223 K (950 °C), the SRX kinetics is very slow and achieves only fractional softening of ~40 pct even after holding for 600 seconds. It is well known from low-C microalloyed steels that the range of maximum effectiveness for Nb atoms is between 1223 K and 1123 K (950 °C and 850 °C). Hence, it can be assumed that the precipitation of NbC carbide, which may be enhanced by concurrent deformation, increases the strain hardening and impedes the SRX kinetics.[38] However, the SRX kinetics is enhanced as the temperature increases beyond about 1223 K (950 °C) and sigmoidal Avrami-type curves can be fitted reasonably with the experimental data. The scatter in the data can be tentatively attributed to the heterogeneity (segregation bands) and also nonuniformity of grain structure noticed in some areas. Data obtained on specimens reheated at 1523 K (1250 °C) for 5 minutes to produce coarser grains (240 μm) and tested at 1323 K (1050 °C)/0.2/0.1 s^{-1} are also shown in Figure 5(b), which clearly reveals the retardation of recrystallization rate (t_{50} = 33 seconds) in comparison with the finer grained structure (90 μm: t_{50} = 20 seconds). The Avrami exponent (n) has been estimated to be ranging from 0.8 to 0.9 for both steels. It was observed earlier that the Avrami exponent decreased with the decreasing temperature for an Fe-25Mn-1Al steel [1.2, 1.1, 0.8, 0.7, and 0.7 at 1373 K, 1323 K, 1273 K, 1223 K, and 1173 K (1100 °C, 1050 °C, 1000 °C, 950 °C, and 900 °C, respectively)] possibly due to intense dynamic recovery, typical
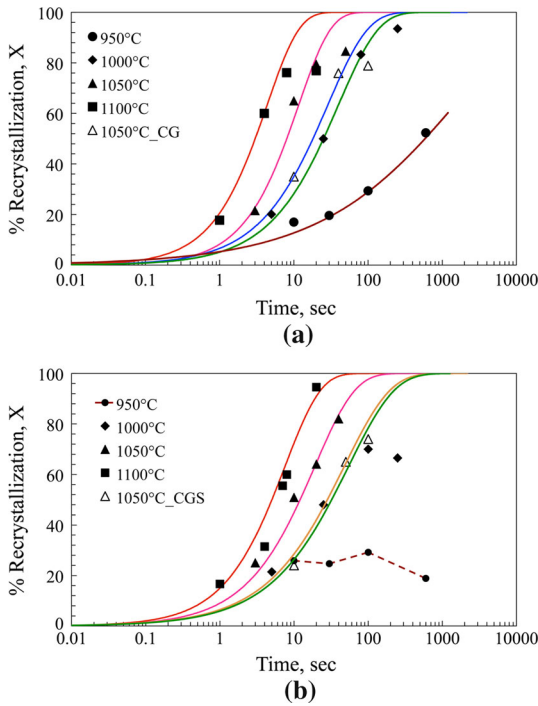
Fig. 7—t_{50} times *vs* the inverse absolute temperature for the determination of the apparent activation energy of SRX for different TWIP steels.

Fig. 6—Double-hit compression data fitted with Avrami-type curves showing SRX rates of steels (*a*) TKSE 16 and (*b*) TKSE 18 at different temperatures following deformation to 0.2 strain at 0.1 s^{-1}.

of TWIP steels with different levels of Al and hence, higher stacking fault energies.[9]

Similarly, characterization of SRX behaviors of two high-V-microalloyed steels with different levels of Al, *viz.*, TKSE 16 and 18, was carried out at different temperatures ranging from 1223 K to 1373 K (950 °C to 1100 °C), as shown in Figure 6. At 1223 K (950 °C), V too has a significant influence on the SRX kinetics of the two steels possibly due to precipitation that impedes the recrystallization process (for instance, 50 pct fractional softening after holding for ~600 seconds in the case of TKSE 16). However, the SRX rate was enhanced as the temperature increased beyond 1223 K (950 °C) [reasonable as VC dissolution temperature ≈1238 K to 1243 K (965 °C to 970 °C), Table I] and the SRX kinetics of Steel 16 (0.2V-1.5Al) were then comparable with TKSE 4 suggesting only a small effect of V in solution on the softening of this steel, Figure 6(a). The effect of V on the SRX kinetics of carbon steels too has been known to be small, when compared with Nb and Ti.[18] However, with the increasing Al content to 4.9 pct in TKSE 18, the kinetics were further retarded, and the SRX rates were slower than those of TKSE 16 despite comparable grain sizes (about 120 μm), Figure 6(b). All the same, both V-microalloyed steels (TKSE 16 and 18) as well as the reference steel (TKSE 4) showed significantly faster softening compared with Nb-microalloyed TKSE 12, as will be discussed later. In addition, it has been noticed that Avrami-type fits were sometimes not quite good at high recrystallized fractions, particularly in the case of microalloyed TWIP steels. As illustrated above, in the double-hit compression technique, the flow stress of
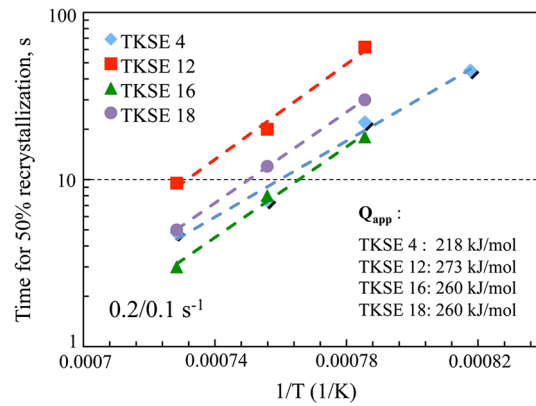
recrystallized material, σ_1, is conventionally taken from the first pass. At times, this may indicate low recrystallized fraction because the flow stress of the second pass may not restore to the level of the first pass and may remain slightly higher even after complete recrystallization, presumably due to machine effects or grain size refinement.[22]

The Avrami exponents of the high-V steels were found to be ranging from 0.7 to 1.0, which are comparable with other TWIP steels reported earlier.[9,28,31]

2. Apparent activation energy of recrystallization (Q_{app})

For a given set of experimental conditions, *viz.*, strain, strain rate, and grain size, Eq. [4] can be rewritten as

$$\ln(t_{50}) = K + Q_{app}/RT, \qquad [7]$$

where K is a constant ($= \ln[A' \, \varepsilon^p \, \varepsilon'^q \, d^s]$). The slopes of the $\ln(t_{50})$ *vs* 1/T (inverse absolute temperature) plots can, therefore, be used to compute the Q_{app} values for different steels, *i.e.*, $Q_{app} = R \times$ slope. The temperature dependence of SRX kinetics for all TWIP steels is shown in Figure 7, where t_{50} times estimated at different temperatures for specimens deformed to 0.2 strain at 0.1 s^{-1} are plotted against the inverse absolute temperature. The apparent activation energies of SRX deduced from the data are about 218, 273, 260, and 260 kJ/mol for steels TKSE 4, 12, 16, and 18, respectively. Earlier, a value of 257 kJ/mol was estimated for the Nb-free Fe-25Mn-1Al TWIP steel.[9] The Q_{app} values for C-Mn (184 kJ/mol) and C-Mn-Nb (230 kJ/mol) steels[18] further reveal the significant effect of Nb on Q_{app} in Nb-microalloyed TKSE 12 TWIP steel (273 kJ/mol). The Q_{app} values of microalloyed TWIP steels are comparable with both 12Cr (265 kJ/mol) and Type 304 (283 kJ/mol) steels, for instance.[34] All these values are of the same order and can be considered reasonable, despite the fact that the estimates of Q_{app} values are based on limited double-hit compression data with considerable scatter. In contrast with the above, Wu *et al.*[39] calculated a very low value of 147 kJ/mol for
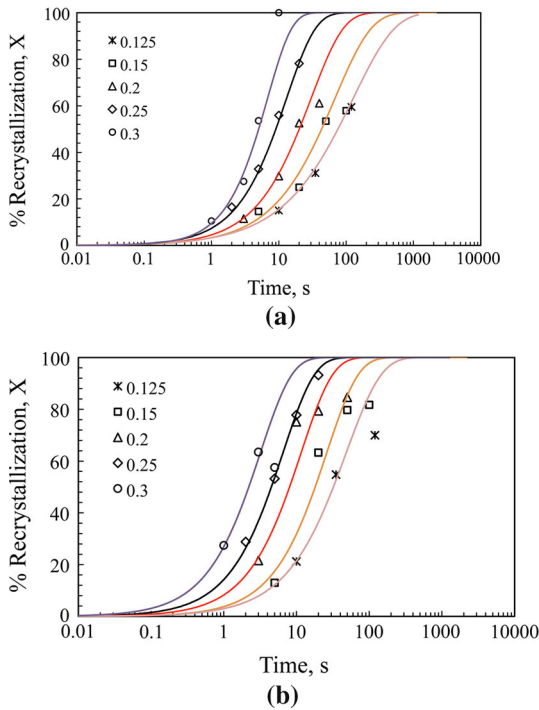
Fig. 8—Double-hit compression data fitted with Avrami-type curves showing effect of strain on SRX rates of steels TKSE 12 (*a*) and TKSE 16 (*b*) following deformation at 1323 K (1050 °C)/0.1 s^{-1} to different strains.
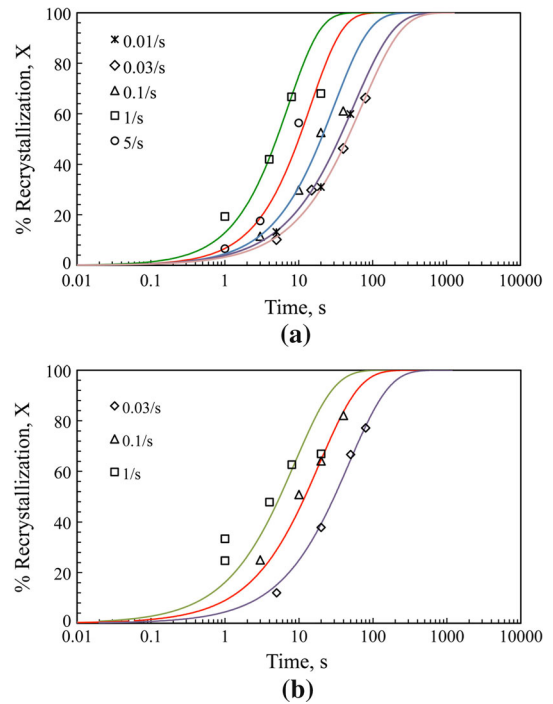
Fig. 9—Double-hit compression data fitted with Avrami-type curves showing effect of strain rate on SRX rates of steels TKSE 12 (*a*) and TKSE 18 (*b*) following deformation at 1323 K (1050 °C) to a true strain of 0.2 at different strain rates.

SRX activation energy. Presumably, the recrystallization in their tests was of metadynamic type and not static one, as the apparent activation energy of metadynamic recrystallization has been shown to be low.[18,22,34,40]

Referring to Figure 7, the SRX rate of Nb-bearing TKSE 12 (average grain size 90 μm) is much slower compared with the reference steel TKSE 4 (average grain size 160 μm) as well as the high-V TKSE 16 (average grain size 110 μm). TKSE 18 with 4.9 pct Al and having comparable grain size (120 μm) showed somewhat slower kinetics, but much faster than that of TKSE 12.

3. Powers of strain and strain rate

Some examples of the effect of strain on the SRX kinetics at a given temperature 1323 K (1050 °C) and strain rate 0.1 s^{-1} are shown in Figures 8(a) and (b). It can be seen that with the increasing strain, the SRX rate increases significantly and the corresponding Avrami curves shift to lower times. Overall, no distinct trend in the Avrami exponent (*n*) as a function of strain is discernible due to scatter in the data; however, *n* seemed to increase with the strain in the case of TKSE 12.

The influences of strain rate on the SRX kinetics are shown in Figures 9(a) and (b). Recrystallized fractions were estimated from the double-hit compression curves of specimens deformed at 1323 K (1050 °C) to a true strain of 0.2 at different strain rates ranging from 0.01 to 5 s^{-1}. It can be seen that a higher strain rate enhances the SRX kinetics owing to reduced dynamic recovery,

even though the influence of strain rate is much lower in comparison with strain. Due to scatter in data, there was no clear trend in respect of Avrami exponent (*n*), which varied in a narrow range.

The effects of strain and strain rate on t_{50} times for different TKSE steels are displayed in Figures 10(a) and (b). The powers of strain (*p*) and strain rate (*q*) are estimated based on the plots of (i) t_{50} *vs* strain at 1323 K (1050 °C)/0.1 s^{-1} (Figure 10(a)), and (ii) t_{50} *vs* strain rate at 1323 K (1050 °C)/0.2 strain (Figure 10(b)), respectively.

As can be discerned from Figure 10(a), the slopes of the line fits are quite similar for both steels, and the power of strain (*p*) was estimated to be about −3.0 for both the reference (TKSE 4) as well as microalloyed TWIP steels (TKSE 12, 16, and 18), and this value is very close to that reported for an ordinary 25Mn1Al TWIP steel (−2.8).[9] Similarly, the power of strain rate (*q*) was estimated to vary in a narrow range −0.3 to −0.34, estimated from the slopes of the line fits irrespective of the steel type. The trend is similar to that reported earlier for 25Mn1Al steel −0.30.[9]

The strain exponents for ordinary C-Mn steels have been reported to be ranging from −2.5 to −4.[18,19,22,41,42] Values between −2 and −3 were measured by the stress relaxation technique for some microalloyed steels.[18,19,22,43] Values of −2.8 and −2.5 for the strain exponent have been used by Somani et al.[18] for C/C-Mn/Nb/Ti/Nb-Ti and Mn-V steels, respectively. Hamada et al.[9] used a value of −2.7 for ordinary TWIP steels and Karjalainen et al.[34]
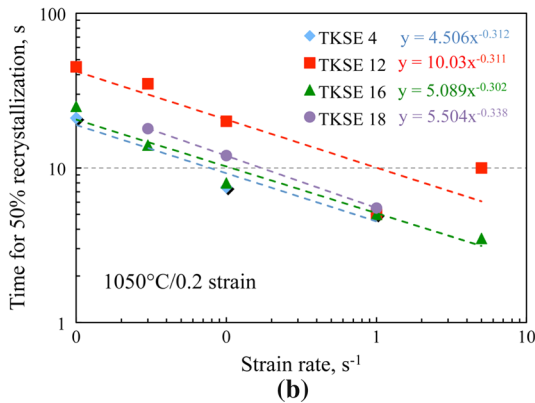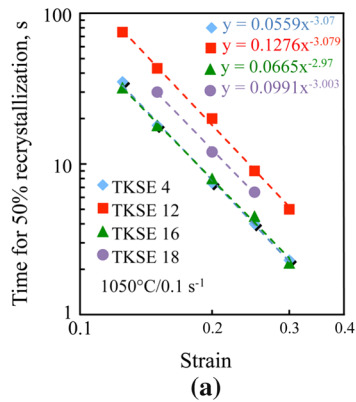
(a)

(b)

Fig. 10—Plots of (a) t_{50} vs strain at 1323 K (1050 °C)/0.1 s^{-1} and (b) t_{50} vs strain rate at 1323 K (1050 °C)/0.2 strain for different TKSE steels.

determined values of −3.0 and −1.5 for Type 304 and 12Cr stainless steels, respectively. All these values are of the same order, and hence, the measured estimates of −2.97 to −3.08 (Figure 10(a)) for the present TWIP steels can be considered reasonable.

Based on the limited experimental data, the power of strain rate for a 25Mn1Al TWIP steel and some other Fe-25Mn-(0-6)Al steels was determined to be −0.3.[9] Karjalainen *et al.*[34] reported values of −0.30 and −0.33 for Type 304 and 12Cr stainless steels, respectively. In comparison, relatively lower values of −0.11 and −0.12 have been reported for C/C-Mn and Ti steels.[18,19,44] As intermediate between these two groups, the strain rate exponents for Nb and Nb-Ti and also Mo-steels have been estimated to be of the order of −0.23.[18] All these values fall within a reasonably narrow range (−0.11 to −0.34) indicating a weak dependence of SRX on strain rate irrespective of the steel alloying and the strain rate exponents ranging from −0.3 to −0.34 (Figure 10(b)) for the present TWIP steels in this study is in line with the exponents for ordinary Mn-Al TWIP, Type 304 and 12Cr steels.

4. Fractional softening equations for SRX

Taking the power of grain size (*s*) to be described by the following relation $s = 2.13d^{-0.105}$ proposed by Somani *et al.*,[18,19] as also used for Fe-25Mn-Al TWIP steels,[9] together with the above values for the

other parameters (Q_{app}, *p* and *q*) in Eq. [4] gives the constant A' for different TWIP steels. The SRX rates of different TKSE steels can be reasonably described by the following SRX equations:

TKSE 4:

$$t_{50} = 1.41 \times 10^{-13} \varepsilon^{-3.07} \dot{\varepsilon}'^{-0.312} d^s \exp(218{,}000/RT), \quad [8]$$

TKSE 12:

$$t_{50} = 3.11 \times 10^{-15} \varepsilon^{-3.08} \dot{\varepsilon}'^{-0.311} d^s \exp(273{,}000/RT), \quad [9]$$

TKSE 16:

$$t_{50} = 4.34 \times 10^{-15} \varepsilon^{-2.97} \dot{\varepsilon}'^{-0.302} d^s \exp(260{,}000/RT), \quad [10]$$

TKSE 18:

$$t_{50} = 5.07 \times 10^{-15} \varepsilon^{-3.0} \dot{\varepsilon}'^{-0.338} d^s \exp(260{,}000/RT), \quad [11]$$

where[18,19]

$$s = 2.13 \, d^{-0.105}. \quad [12]$$

While formulating the above equations, enough care has been taken to ignore the data, which were close to peak strains. Equation [12][18,19] was previously determined based on the SRX data of a large number of carbon steels (both non-microalloyed and microalloyed grades) and has since been found to work reasonably well with TWIP steels also.[9,28] Hence, it has now been extended to the current reference TWIP steel (TKSE 4) and other microalloyed TWIP steels (TKSE 12, 16, and 18), too.

In order to check the reliability of the fractional softening equations (Eqs. [8] through [11]), a few confirmation experiments were carried out by varying deformation parameters [1298 K (1025 °C)/0.18/ 0.05 s^{-1} and 1348 K (1075 °C)/0.15/0.5 s^{-1}] and/or using a coarser grain size obtained by reheating at 1523 K (1250 °C) for 5 minutes (see Table II) followed by deformation at 1323 K (1050 °C)/0.2/0.1 s^{-1}. Figures 11(a) and (b) presents examples of the plots of experimental *vs* predicted t_{50} values for all deformation conditions. It can be seen that the agreement between the experimental and predicted values is quite satisfactory. Data from confirmation tests for validation are also included in the figures. This indicates that the above modeling equations for the four TWIP steels give an accurate prediction of their respective SRX kinetics. In any case, the strain rates used in these experiments are relatively low compared to those experienced in plate and sheet hot rolling. Also, the equation describing the power of grain size (*s*; Eq. [12]) was found to be reasonable for these microalloyed TWIP steels, too, at least for the large grain sizes in these experiments.
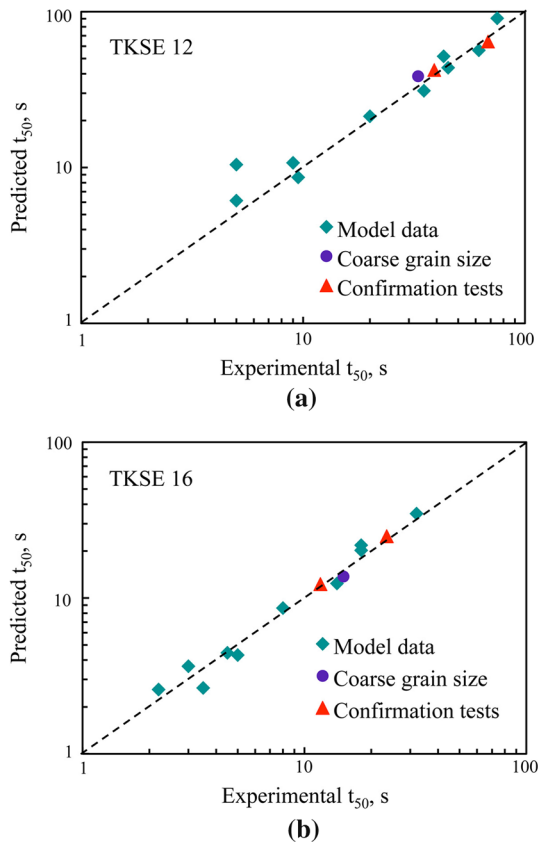
Fig. 11—Plots of predicted *vs* experimental t_{50} data (*a*) TKSE 12 and (*b*) TKSE 16. Data from confirmation experiments are also included.

5. Microstructural analysis for validation of SRX fractional softening equations

In TWIP steels, there is no phase transformation upon cooling so that it is also possible to determine SRX fractions metallographically. In this respect, the SEM-EBSD technique even allows for the distinction between recrystallized (sub-boundary free) grains and recovered (sub-boundaries containing) grains and thereby allows for the validation of the fractional softening approach. As examples, a few recrystallized fractions determined for the Nb-bearing TKSE 12 specimens deformed at 1373 K (1100 °C) to a strain of 0.2 at 0.1 s^{-1} are presented here. Recrystallized fractions were determined from the recorded EBSD orientation maps using the Tango® program, which allows the deformed and recrystallized fractions to be estimated. The misorientation angle used to define the high-angle grain boundaries was taken as 15 deg, and the misorientation measurements were recorded down to 2 deg. Twin boundaries with the tolerance of ±2 deg for 60 deg misorientation at about $\langle 111 \rangle$ rotation axis were not regarded as the grain boundaries. The program measures the internal average misorientation angle within each grain. If the average misorientation of the boundaries in a grain exceeds a user-defined minimum angle to define a subgrain, θ, the grain is classified as "deformed." All the remaining grains are classified as "recrystallized."
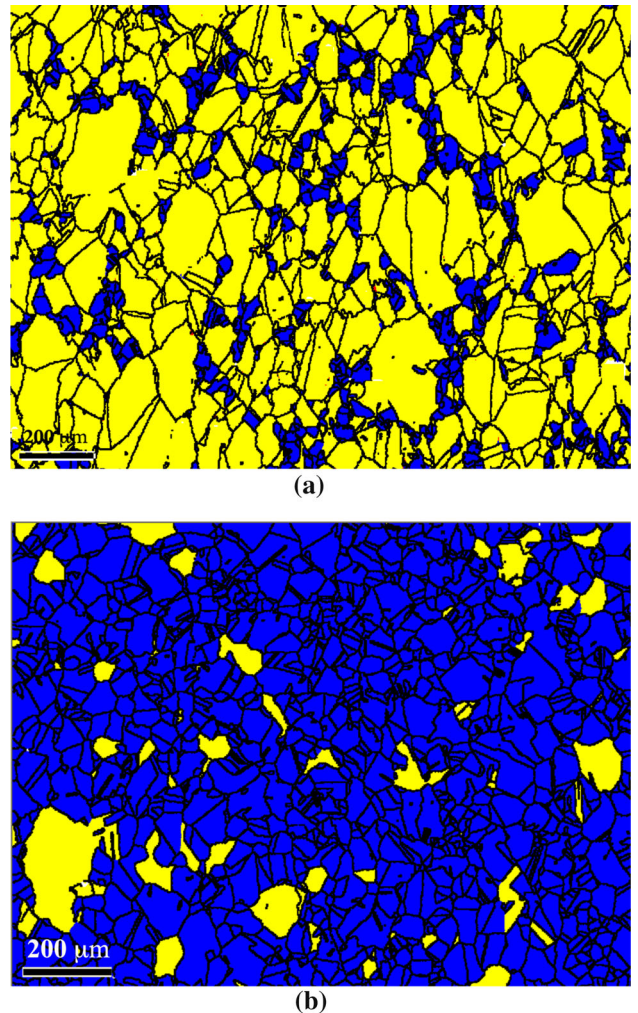

Fig. 12—EBSD microstructures of TKSE 12 steel deformed at 1373 K (1100 °C) to a strain of 0.2 at 0.1 s^{-1} showing deformed (yellow) and recrystallized (blue) grains following holding for (*a*) 2 s and (*b*) 30 s, respectively.

The misorientations of low-angle grain boundaries in the substructure vary ranging from 2 to 5 deg. A threshold value of 2.5 deg was chosen for the value of θ. On that basis, deformation with ε: 0.2, ε': 0.1 s^{-1}, and subsequent holding times for 2 and 30 s at 1373 K (1100 °C) gave of 16 and 90 pct recrystallization, respectively. Figure 12 shows the partly recrystallized microstructures obtained using the SEM-EBSD method, showing recrystallized (blue) and deformed (recovered) grains (yellow). The corresponding softening fractions calculated from the Eq. [9] are 17 and 88 pct, respectively, thus confirming the validity of the fractional softening equation as well as the reliability of the double-hit compression technique in determining the recrystallization fractions.

6. SRX behavior and activation energy of recrystallization

A summary of the powers of strain and strain rate, deformation activation energy, and apparent and recrystallization activation energies (Q_{app} and Q_{rex},

Table V.   A Summary of Powers of Strain (p) and Strain Rate (q), Activation Energy of Deformation (Q_{def}) as Well as Apparent and Recrystallization Activation Energies (Q_{app} and Q_{rex})

Steel	Brief Composition	p	q	Q_{def}	Q_{app}	Q_{rex}	References
C-Mn-Nb	0.15C-0.3Si-1.4Mn-0.033Nb	−2.8	−0.23	400	280	372	[18]
Type 304 SS	0.03C-0.44Si-1.5Mn-18.3Cr-8.6Ni-0.13Mo	−3.0	−0.3	410	283	406	[34]
25Mn1Al	Fe-26Mn-0.43Cr-0.4Si-0.16C-1Al	−2.7	−0.3	385	257	373	[3]
TKSE 4	Fe-20Mn-1.5Al-0.6C	−3.07	−0.312	388	218	339	present work
TKSE 12	Fe-20Mn-1.5Al-0.6C-0.026Nb	−3.08	−0.311	402	273	398	present work
TKSE 16	Fe-20Mn-1.5Al-0.6C-0.3V	−2.97	−0.302	404	260	382	present work
TKSE 18	Fe-20Mn-5Al-0.6C-0.3V	−3.0	−0.338	422	260	403	present work

respectively) obtained for the four TKSE steels is presented in Table V in comparison with other steel grades such as microalloyed C-Mn-Nb, Type 304 stainless steel, and Fe-25Mn-1Al steel. Q_{rex} has been computed using the following equation[21]:

$$Q_{rex} = Q_{app} - q \cdot Q_{def}. \qquad [13]$$

As can be seen from Table V, the strain exponent varies in a narrow range between −2.7 and −3.1. All these values are of the same order and can be considered reasonable. Similarly, the strain rate exponent for microalloyed TWIP steels varies in a very narrow range (−0.3 to −0.34). The power of strain rate for the current steels is in line with the exponents for 25Mn1Al and Type 304 stainless steel and slightly above that of Nb-microalloyed C-steel (−0.23). The low value of strain rate exponent indicates a weak dependence of SRX on strain rate irrespective of the steel alloying.

Except for slightly low Q_{def} for non-microalloyed reference composition (TKSE 4; 388 kJ/mol), which is comparable with Fe-25Mn-1Al steel (385 kJ/mol, Table V), all microalloyed steels showed Q_{def} in a narrow range (402 to 422 kJ/mol), in line with those of Nb-microalloyed and Type 304 stainless steel grades. As mentioned earlier, Al ranging from 5 to 6 pct is known to increase the flow stress and Q_{def}, beyond which there is a significant drop due to manifestation of δ-ferrite in the microstructure.[8,9,31,45]

The Q_{app} value of SRX varies in a wide range (218 to 273 kJ/mol) for these steels (Table V). Except for the reference steel TKSE 4, the Q_{app} values for microalloyed steels (TKSE 12, 16, and 18) are in the same range as reported for 25Mn1Al TWIP, C-Mn-Nb, and 304 stainless steel grades depending on the type and extent of alloying. While microalloying with Nb seems to have a large effect on Q_{app}, alloying with V seems to have only a marginal effect. Despite varying Al contents in 0.3 V-bearing TKSE 16 (1.5 pct) and TKSE 18 (4.9 pct) steels, the Q_{app} value remains unchanged suggesting practically no effect of Al on Q_{app}. Since, both the power of strain rate (q) and Q_{def} vary in a narrow range, the data of activation energies of recrystallization (Q_{rex}) for microalloyed TWIP steels TKSE 12, 16, and 18 computed using Eq. [13] show a trend similar to Q_{app} (see Table V). The Q_{app} and also the Q_{rex} values (218 and 339 kJ/mol, respectively) for the reference steel seem somewhat low in comparison with the value earlier determined for 25Mn1Al steel with slightly higher Mn content (257 and 373 kJ/mol, respectively; Table V).
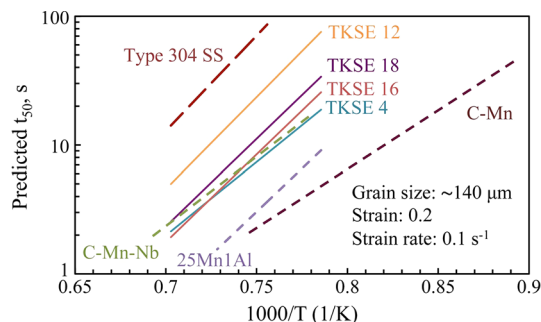

Fig. 13—t_{50} vs inverse absolute temperature for various TWIP steels in comparison with other steels.

The times for 50 pct recrystallized fraction (t_{50}) estimated for the TKSE steels by using the fractional softening equations derived above (Eqs. [8] through [11]) for a strain of 0.2 at 0.1 s^{-1} and a grain size of 140 μm are shown in Figure 13. Corresponding t_{50} vs inverse absolute temperature plots for C-Mn, Nb-microalloyed C-Mn-Nb, and Type 304 stainless steel are also included in the figure. As expected, C-Mn steel exhibits the fastest recrystallization rate, while Type 304 stainless steel showed the slowest rate. On the other hand, the rate of SRX in high-Mn steels used in the current study seems to be markedly slower than in a low-Mn carbon (C-Mn) steel. This must be due to the high-Mn content in TWIP steels.

While microalloying with V up to 0.3 pct seems to have little or no effect on the SRX kinetics of TKSE 16 in comparison with reference TKSE 4, the addition of high Al (4.9 pct) in TKSE 18 marginally retarded the SRX kinetics in comparison with TKSE 16 and also TKSE 4. In contrast, Reyes et al.[13] reported that 0.12 pct V did retard the DRX kinetics of a 0.48C-22.5Mn-1.6Al-1.4Si-0.12V-microalloyed TWIP steel. According to the results, V could be useful in controlling the size of the recrystallized grains during hot deformation through a proper rolling schedule design, in addition to precipitation strengthening.

Earlier, Al has been reported to have only a marginal effect on SRX kinetics of TWIP steels.[9] All these three steels (TKSE 4, 16, and 18) have comparable recrystallization behaviors with the ordinary Nb-microalloyed low-Mn carbon (C-Mn-Nb) steel, Figure 13. On the other hand, microalloying with 0.026 pct Nb in TKSE TWIP steels significantly slowed down the rate of SRX, as exhibited by TKSE 12, and the corresponding plot

remains somewhere between those of TKSE 18 and Type 304 SS. Hence, Nb seems to have significant retarding effects both for low-Mn and high-Mn steels. The SRX rate of a previously reported Nb-free, 25Mn1Al TWIP steel has also been included in the figure,[9] which lies somewhere between Nb-microalloyed C-Mn-Nb and non-microalloyed C-Mn steels. It is unclear why the SRX rate of 25Mn1Al steel is faster than that of non-microalloyed reference steel TKSE 4 despite the latter having lower Mn content (20 pct).

IV. SUMMARY AND CONCLUDING REMARKS

The constitutive flow and recrystallization behaviors of Nb- or V-microalloyed Al-bearing high-Mn TWIP steels have been evaluated. A large number of single- and double-hit compression tests at high temperatures enabled determination of the activation energies Q_{def} and Q_{rex}, besides evaluating the powers of strain and strain rate for developing fractional softening equations. The results can be summarized as follows:

In line with the literature, Al increases the flow stress as well as Q_{def} of high-Mn steels and delays the onset of DRX thus influencing the peak stress behavior. In contrast, microalloying additions in solution do not show any discernible effect on the flow stress level, although they increase the Q_{def} of high-Mn steels marginally. The influence on peak stress behavior was, however, not detectable.

Except for somewhat lower Q_{def} of the non-microalloyed composition (TKSE 4; 388 kJ/mol), all other steels showed Q_{def} in a narrow range (402 to 422 kJ/mol) with Nb and V having an identical effect (Q_{def} 402 and 404 kJ/mol for TKSE 12 and 16, respectively) and high Al (4.9 pct) augmenting it to a slightly higher value (422 kJ/mol; TKSE 18).

Double-hit compression tests have been suitably employed for determining the fractional softening equations for SRX in microalloyed TWIP steels; the influences of temperature and grain size on SRX behavior were clearly revealed and appropriately modeled.

Powers of strain ($p \approx -2.97$ to -3.08) and strain rate ($q \approx -0.3$ to -0.34) varied in a narrow range and are comparable with austenitic stainless steels and other TWIP steels.

Microalloying additions, particularly Nb, have a discernible effect on the Q_{app} values of microalloyed TWIP steels (273, 260, and 260 kJ/mol for TKSE 12, 16, and 18 steels, respectively) in comparison with non-microalloyed TKSE steel (218 kJ/mol) and comparable to those reported for 12Cr (265 kJ/mol) and Type 304 (283 kJ/mol) steels.

Since the powers of strain and strain rate, and the Q_{def} values vary in a narrow range, the Q_{rex} data of microalloyed TWIP steels (TKSE 12, 16, and 18) too showed a trend similar to Q_{app} and varied in a narrow range (382 to 403 kJ/mol), but were much higher than that of the non-microalloyed TKSE 4 steel (339 kJ/mol).

Confirmation experiments suggest the reasonability of the fractional softening equations developed for different microalloyed TWIP steels; the equation for power of

grain size (s) suggested by Somani et al.[18,19] has been found to be suitable for these steels, too, at least for large grain sizes.

Microalloying with V up to 0.3 pct seems to have little or no effect on the SRX kinetics in comparison with non-microalloyed TWIP steel, and the kinetics are comparable with ordinary Nb-microalloyed carbon steels. Addition of high Al (4.9 pct) marginally retarded the SRX rate in comparison with the steels with low Al (1.5 pct). However, microalloying with Nb significantly slowed down the SRX kinetics, thus suggesting that Nb has significant influence on high-Mn steels, similarly as in the case of plain C-Mn steels. All the same, its rate is still somewhat faster than that of Type 304 steel.

REFERENCES

1. O. Grassel, L. Kruger, G. Frommeyer, and L.W. Meyer: *Int. J. Plast.*, 2000, vol. 16, pp. 1391–1409.
2. G. Frommeyer, U. Brüx, and P. Neumann: *ISIJ Int.*, 2003, vol. 43, pp. 438–46.
3. O. Bouaziz, S. Allain, C.P. Scott, P. Cugy, and D. Barbier: *Curr. Opin. Solid State Mater. Sci.*, 2011, vol. 15, pp. 141–68.
4. J.P. Chateau, A. Dumay, S. Allain, and A. Jacques: *Proceedings of the 15th International Conference on Strength of Materials (ICSMA-15)*, *J. Physics: Conf. Series*, 2010, vol. 240, p. 012023. DOI: 10.1088/1742-6596/240/1/012023.
5. C. Scott, B. Remy, J.-L. Collet, A. Cael, C. Bao, F. Danoix, B. Malard, and C. Curfs: *Int. J. Mater. Res.*, 2011, vol. 102, pp. 538–49.
6. Project PrecHiMn, *Precipitation in High Manganese Steels*, Annual Report, Research Fund for Coal and Steel (RFCS), European Commission, Brussels, 2014.
7. A.S. Hamada, L.P. Karjalainen, and M.C. Somani: *Mater. Sci. Eng. A*, 2007, vol. 467, pp. 114–24.
8. A.S. Hamada, L.P. Karjalainen, and M.C. Somani: *Cand. Metall. Quart.*, 2007, vol. 46, pp. 47–56.
9. A.S. Hamada, L.P. Karjalainen, and M.C. Somani: *ISIJ Int.*, 2007, vol. 47, pp. 907–12.
10. D. Li, Y. Feng, Z. Yin, F. Shangguan, K. Wang, Q. Liu, and F. Hu: *Mater. Sci. Eng. A*, 2011, vol. 528, pp. 8084–89.
11. A. Marandi, A. Zarei-Hanzaki, N. Haghdadi, and M. Eskandari: *Mater. Sci. Eng. A*, 2012, vol. 554, pp. 72–78.
12. J. Zhang, H. Di, X. Wang, Y. Cao, J. Zhang, and T. Ma: *Mater. Des.*, 2013, vol. 44, pp. 354–64.
13. F. Reyes, J. Calvo, J.M. Cabrera, and I. Mejía: *Steel Res. Int.*, 2012, vol. 83, pp. 334–39.
14. L.A. Dobrzański and W. Borek: *J. Achiev. Mater. Manufact. Process.*, 2011, vol. 46, pp. 71–78.
15. L.A. Dobrzański and W. Borek: *Mater. Sci. Forum*, 2012, vols. 706–709, pp. 2053–58.
16. M. Schinhammer, C.M. Pecnik, F. Rechberger, A.C. Hänzi, J.F. Löffler, and P.J. Uggowitzer: *Acta Mater.*, 2012, vol. 60, pp. 2746–56.
17. C.M. Sellars and W.J.McG. Tegart: *Int. Met. Rev.*, 1972, vol. 17, pp. 1–16.
18. M.C. Somani, L.P. Karjalainen, D.A. Porter, and R.A. Morgridge: in *Proceedings of the International Conference on Thermomechanical Processing: Mechanisms, Microstructure and*

Control, E.J. Palmiere, M. Mahfouf, and C. Pinna, eds., The University of Sheffield, Sheffield, 2003, pp. 436–41.

19. M.C. Somani and L.P. Karjalainen: *Mater. Sci. Forum*, 2012, vols. 715–716, pp. 751–56.

20. B. Roebuck, J.D. Lord, R.K. Varma, and M.S. Loveday: *Guidelines for the Measurement of Flow Stress in Hot Axisymmetric Compression Tests, NPL Report CMMT(BPG)003*, National Physical Laboratory, Middlesex, 1997.

21. J.S. Perttula and L.P. Karjalainen: *Mater. Sci. Technol.*, 1998, vol. 14, pp. 626–30.

22. J. Perttula: Ph.D. Thesis, Acta Universitatis Ouluensis, C 119, University of Oulu, Finland, 1998.

23. C. Scott, and P. Cugy: *Proceedings of the International Symposium on Automobile Steel (ISAS'09)*, Dalian, China, 2009, pp. 211–21.

24. Thermo-Calc Software AB: TCFE6—TCS Steel/Fe-Alloys Database, Version 6.2, 2010.

25. K.-T. Park, S.W. Hwang, J.H. Ji, and C.S. Lee: *Proc. Eng.*, 2011, vol. 10, pp. 1002–06.

26. H.J. McQueen, S. Yue, N.D. Ryan, and E. Fry: *J. Mater. Process. Technol.*, 1995, vol. 53, pp. 293–310.

27. F. Reyes-Calderón, I. Mejia, A. Boulaajaj, and J.M. Cabrera: *Mater. Sci. Eng. A*, 2013, vol. 560, pp. 552–60.

28. M.C. Somani, H. Tervonen, L.P. Karjalainen, and D.A. Porter: *Mater. Sci. Forum*, 2013, vol. 753, pp. 195–200.

29. F. Reyes-Calderón, I. Mejía, and J.M. Cabrera: *Mater. Sci. Eng. A*, 2013, vol. 562, pp. 46–52.

30. M. El Wahabi, J.M. Cabrera, and J.M. Prado: *Mater. Sci. Eng. A*, 2003, vol. 343, pp. 116–25.

31. A.S. Hamada: Ph.D. Thesis, Acta Universitatis Ouluensis, C 281, University of Oulu, Finland, 2007.

32. D. Li, Y. Feng, Z. Yin, F. Shangguan, K. Wang, Q. Liu F. Hu: *Mater. Des.*, 2012, vol. 34, pp. 713–18.

33. W. Xiong, B. Wietbrock, A. Saeed-Akbari, M. Bambach G. Hirt: *Steel Res. Int.*, 2011, vol. 82, pp. 127–36.

34. L.P. Karjalainen, J.A. Koskiniemi, and X.D. Liu: *Proceedings of the 37th Mechanical Working and Steel Processing Conference & International Symposium on Recovery and Recrystallization in Steel*, Hamilton, ON, 1995, vol. XXXIII, pp. 861–69.

35. D.J. Towle and T. Gladman: *Met. Sci.*, 1979, vol. 13, pp. 246–56.

36. G. Mohapatra and S.S. Sahay: *Mater. Sci. Technol.*, 2011, vol. 27, pp. 377–81.

37. C.M. Sellars and J.A. Whiteman: *Met. Sci.*, 1979, vol. 13, pp. 187–94.

38. L.M. Fu, H.R. Wang, W. Wang, and A.D. Shan: *Mater. Sci. Technol.*, 2011, vol. 27, pp. 996–1001.

39. Y.X. Wu, D. Tang, Z.L. Mi, and H.T. Jiang: *Adv. Mater. Res.*, 2014, vol. 893, pp. 419–23.

40. L.P. Karjalainen and J.S. Perttula: *ISIJ Int.*, 1996, vol. 36, pp. 729–36.

41. P.D. Hodgson and R.K. Gibbs: *ISIJ Int.*, 1992, vol. 32, pp. 1329–38.

42. C.M. Sellars: *Mater. Sci. Technol.*, 1990, vol. 6, pp. 1072–81.

43. L.P. Karjalainen: *Proceedings of the 3rd International Conference on HSLA Steels*, The Chinese Society for Metals, Beijing, 1995, pp. 179–84.

44. K. Airaksinen, L.P. Karjalainen, D. Porter, and J. Perttula: *Mater. Sci. Forum*, 1998, vols. 284–286, pp. 119–26.

45. A.S. Hamada, L.P. Karjalainen, M.C. Somani, and R.M. Ramadan: *Mater. Sci. Forum*, 2007, vol. 550, pp. 217–22.